Sea-Island Polyurethane/Polycarbonate Composite Nanofiber Fabricated Through Electrospinning

Ruilai Liu,[1] Ning Cai,[1] Wenqing Yang,[1] Weidu Chen,[2] Haiqing Liu[1,3]

[1]*College of Chemistry and Materials Science, Fujian Normal University, Fuzhou 35007, China*
[2]*School of Chemistry and Chemical Engineering, Sun Yat-sen University, Guangzhou 510275, China*
[3]*Fujian Key Laboratory of Polymer Materials, Fuzhou 350007, China*

Received 23 February 2009; accepted 2 October 2009
DOI 10.1002/app.31539
Published online 23 December 2009 in Wiley InterScience (www.interscience.wiley.com).

ABSTRACT: Sea-island polyurethane (PU)/polycarbonate (PC) composite nanofibers were obtained through electrospinning of partially miscible PU and PC in 3 : 7 (v/v) *N*,*N*-dimethylformamide (DMF) and tetrahydrofuran (THF) mixture solvent. Their structures, mechanical, and thermal properties were characterized by scanning electron microscopy (SEM), transmission electron microscopy (TEM), Fourier transform infrared (FTIR) spectroscopy, thermogravimetric (TG), and differential scanning calorimetry (DSC). The structures and morphologies of the nanofibers were influenced by composition ratio in the binary mixtures. The pure PC nanofiber was brittle and easy to break. With increasing the PU content in the PU/PC composite nanofibers, PU component not only facilitated the electrospinning of PC but improved the mechanical properties of PU/PC nanofibrous mats. In a series of nanofibrous mats with varied PU/PC composition ratios, PU/PC 70/30 showed excellent tensile strength of 9.60 Mpa and Young's modulus of 55 Mpa. After selective removal of PC component in PU/PC composite nanofibers by washing with acetone, the residual PU maintained fiber morphology. However, the residual PU nanofiber became irregular and contained elongated indents and ridges along the fiber surface. PU/PC composite fibers showed sea-island nanofiber structure due to phase separation in the spinning solution and in the course of electrospinning. At PC content below 30%, the PC domains were small and evenly dispersed in the composite nanofibers. As PC content was over 50%, the PC phases became large elongated aggregates dispersed in the composite nanofibers. © 2009 Wiley Periodicals, Inc. J Appl Polym Sci 116: 1313–1321, 2010

Key words: composites; differential scanning calorimetry; fibers; polycarbonates; polyurethanes

INTRODUCTION

One-dimensional (1D) nanostructures have been a subject of intensive research because of their unique properties and intriguing applications in many areas.[1,2] The fabrication of polymer fibers with diameter ranging from several microns down to a few tens of nanometers is of considerable interest for various applications. A number of processing techniques, such as drawing, template synthesis, phase separation, self-assembly, and electrospinning, have been used to prepare polymer nanofibers in recent years. Among these methods the electrospinning process seems to be the only method which can be further developed for mass production of one-by-one continuous nanofibers from various polymers. The high surface areas and complex pore structures make nanofibers useful in filters, sensors, biocatalysts, protective clothing, wound dressing, artificial blood vessels, and controlled drug delivery and tissue growth applications.[3–7]

There is always growing interest in the design and preparation of novel composite nanofibers with improved properties. Blending is a highly effective method because it may combine the merits of each component. So far, fabrication techniques such as multiple jet,[8,9] side-by-side,[10,11] coaxial,[12,13] and polymer blends in a cosolvent have been reported.[14,15] According to the distribution of each component in composite, composite nanofibers are divided into two kinds. One type is composed of two kinds of nanofibers formed by individual pure polymers. Techniques such as side-by-side, multiple jet, and coaxial are commonly used to fabricate this kind of composite nanofibers because of a cosolvent is hard to be found for each component. The other type of composite nanofibers is prepared from electrospinning of polymer blends in a cosolvent. Most composite nanofibers of this type consist of two components. If one component is hard to be electrospun

Correspondence to: H. Liu (haiqing.liu@gmail.com).
Contract grant sponsor: National Natural Science Foundation of China; contract grant numbers: 50973019, 50843030.
Contract grant sponsor: Key Project of Natural Science Foundation of Fujian Province; contract grant number: E0620001.

into nanofibers alone such as chitosan and bombyx mori silk, and the other is a good nanofiber-forming polymer such as polyethylene oxide,[16,17] a cosolvent is normally used to fabricate their composite nanofibers by electrospinning. The two components are separated on a nanoscale level in the nanofiber and one obtains either matrix-dispersed or cocontinuous phase morphologies.

Polycarbonate (PC) and polyurethane (PU) are the two main thermoplastic materials. PC is a hard and stiff engineering material. PU is a novel engineering material possessing characteristics of both rubber and plastic. Moon and Farris[18] and Demir et al.[19] prepared aligned PC nanofibers and PU nanofibers, respectively. The PC(shell)/PU(core) composite nanofibers by a coaxial electrospinning process was also reported by Han et al.[12] However, mechanical properties of PC(shell)/PU(core) composite nanofibrous mats are very poor, with σ_b and E of 0.33–0.82 MPa and 6–13 MPa, respectively. Our goal is to use a cosolvent of PU and PC, and fabricate composite nanofibers by the electrospinning technique. PU/PC composite nanofibers are possible to exhibit excellent mechanical strength and relative stable dimensionality compared with a single component PC or PU nanofiber. In this work, the electrospun of PU/PC is studied in terms of composition ratio in the binary mixtures. The structure, morphology, thermal property, and mechanical performance of the PU/PC composites nanofibers are investigated.

EXPERIMENTAL

Materials

Polycarbonate (PC) ($M_n = 5.8 \times 10^4$) was from Shanghai Chemical Company. Elastollan B64D, a polyester-based hydroxyl-terminated polyurethane (PU) ($M_n = 3.2 \times 10^5$) without free —NCO group, was purchased from BASF Company. All materials were used as received.

Electrospinning process

PU/PC blends of 100/0, 70/30, 50/50, 30/70, and 0/100 (w/w) were dissolved in a mixture of *N*,*N*-dimethylformamide (DMF) and tetrahydrofuran (THF) (30/70, v/v) at room temperature to a fixed weight concentration of 18%. It was observed that the miscibility of these two polymers in the solution is poor, because the blend solutions are not completely transparent. No precipitates or bilayers were formed. The PU/PC spinning solution was added to a 10-mL syringe attached to a stainless needle with an inner diameter of 0.84 mm. An electrode was clamped on the needle and connected to a power supply (DW-P303-IAC, Tianjin Dongwen High Voltage Plant, China). The electric field was kept at 15 kV. A grounded counter electrode was attached to a grounded rotating collector wrapped with Al foil. The feeding rate was 10 μL/min monitored by a syringe pump (TS2-60, Longer Precision Pump Co., Baoding, China) and a 14-cm distance between the collector and needle tip. The products were dried under vacuum at 50°C for 10 h to remove any residual solvents.

Removal of PC from PU/PC composite nanofibers

According to the different solubility of PU and PC in acetone, the PC component in the composite nanofibers was selectively removed by immersing the dried composite nanofibrous mats into acetone for 24 h at room temperature. The remained PU nanofibers were washed with acetone three times. Then, the wet nanofibrous mats were vacuum dried at 90°C for 24 h. The weight loss in this process was calculated accordingly.

Characterization

Surface tension was measured by the platinum plate method with a tensiometer (JK99C, Shanghai Zhongchen Digital Technic Apparatus Co.), and the viscosity was measured with a rotational viscometer (NDJ-1, Shanghai Precision and Scientific Instrument Co., China) at 25°C. Electrical conductivity was measured with an electric conductivity meter (G series, CM-40G, TOA Electronics, Japan).

The morphology and diameter of nanofibers were observed by scanning electron microscope (SEM, JEOL JSM-6380LV) and transmission electron microscope (TEM, JEOL JEM-2010). All samples were sputter-coated with gold before SEM observation. For TEM measurement, the fibers were dispersed ultrasonically in ethanol. FTIR spectra were recorded using Thermo-Nicolet 5700 spectrometer. The thermal properties of the nanofibers were measured on a differential scanning calorimeter (DSC TA Q200) under nitrogen atmosphere. Specimen was first heated to 120°C at a heating rate of 20°C/min to eliminate the thermal history. The second scan was recorded at a heating rate of 10°C/min from −50 to 250°C. The glass transition temperature (T_g), the melting temperature (T_m), the deposition temperature (T_d), and the melting enthalpy (ΔH_m) of the PU/PC composite nanofibers were obtained from the thermogram history. The crystallinity degree of PU (χ_c %) in the composite nanofibers was calculated from the melting enthalpy ratio of PU component in the composite to neat PU crystallites.

Thermogravimetric (TG) experiments were performed on a Mettler Toledo TGA 50 instrument. The experiment was carried out by heating from 30 to

500°C under nitrogen atmosphere using a heating rate of 10°C/min.

The tensile strength of the fibrous mats was measured on Twin Column testing machine (LLOYD LR5K) with cross-head speed of 10 mm/min at room temperature. The size of the samples was 70 mm length, 10 mm width, and 20 mm distance between two clamps. Eight replicates were tested for each sample. The average tensile strength at yield (σ_y) and elongation at break (ε_b) were recorded. Young's modulus (E) was calculated using eq. (1) as follows:

$$E = \frac{\sigma}{\varepsilon} \quad (1)$$

where σ and ε are the tensile strength and strain at the initial stretching stage, respectively.

RESULTS AND DISCUSSION

Morphology and structure of PU/PC composite nanofibers

Figure 1 shows SEM images of PU, PC, and PU/PC composite nanofibers. Pure PC nanofibers were cylindrical with rough surfaces [Fig. 1(a)]. In addition, the pure PC nanofibers were brittle and easy to break during handling, as confirmed by the many fibers ends shown in Figure 1(a). Smooth and round PU nanofibers with diameters of 350–400 nm were obtained [Fig. 1(e)]. Meanwhile, it is interesting to find that PU fibers physically adhered together at some sites [pointed by arrows in Fig. 1(e)]. Because of the low evaporation pressure of DMF at ambient condition, DMF evaporates slowly from the PU nanofiber in the short traveling course (14 cm) from the tip to the collector, resulting in some DMF retaining in the fibers. Thus, if the remaining DMF is not removed in time, PU nanofibers are easy to be redissolved and fused together for the closely adjacent PU nanofibers. These bonding sites are favorable for the improvement of mechanical properties of PU nanofibrous mat, which will be discussed in the following section. Similar observations have been found in the preparation of CA/PU and PVA/PU composite nanofibers.[14,20] Figure 1(b–d) shows the morphology of PU/PC composite nanofibers. PU/PC 30/70 nanofibers were slightly flat and continuous. Their surfaces were rough with many chimbs. Similar observation was reported in the preparation of ribbon-shaped nanofibers by Koombhongse et al.[21] In the electrospinning process, fiber skin is quickly formed because of fast solvent evaporation. Atmospheric pressure tends to collapse the tube formed by the skin as the solvent inside the tube evaporates. The circular fiber cross section becomes elliptical and then flat, finally forms a ribbon with a cross-sectional perimeter nearly the same as the perimeter of the jet. However, with further increasing of PU content, the composite nanofibers gradually became round and smooth [Fig. 1(c–e)]. The relationship between the mean diameter of PU/PC composite nanofibers and the PC content in the composite is presented in Figure 1(f). The average diameter of pure PU and PC nanofibers was 370 ± 23 and 748 ± 46 nm, respectively. However, it was about 500 nm for PU/PC composite nanofibers and showed no significant change with the increasing of PC content. This is due to the fiber morphology changing from flat to round. Table I showed solution properties of PU/PC solutions. The solution viscosities increased with the content of PU in blend solutions. Furthermore, the viscosity of pure PU solution was significantly higher than that of the other blend solutions. Doshi and Reneker[4] pointed out that a higher viscosity results in a larger fiber diameter. However, in our work, while the solution viscosities were increased with the content of PU in blend solution, the fiber diameter was decreased. This phenomenon contribute to that PU possesses characteristics of elastomer and can be easily drawn, so the polymer fluid jets may be easily elongated in the electrospinning process. Nevertheless, PC is so stiff that it is hard to be stretched. Therefore, the diameter of PC nanofiber is bigger than that of PU nanofibers although the viscosity of the former solution is quite low.

DSC thermograms of PU/PC composite nanofibers are presented in Figure 2. The glass transition temperature (T_g) of PU and PC appeared at −28.19°C [Fig. 2(e)] and 169.28°C [Fig. 2(a)], respectively. In general, T_g of PU increased slightly with the presence of PC in the composite nanofibers (Table II). Inversely, T_g of PC decreased slightly with the presence of PU in the composite nanofibers (Table II), suggesting that the PC phase may partially miscible with PU in the composite nanofibers. Interaction between PU and PC component through hydrogen bonding is readily formed between carbonyl and amide groups of PU and PC (Scheme 1), which helps improve their miscibility at the interface. The melting temperature (T_m) of PU at ~ 208°C did not vary very much for PU/PC composite nanofibers with various compositions. However, the T_m of PC was not noticeable in the thermograms of PU/PC composite nanofibers, because PC has no obvious melting temperature. Compared with the pure PU fiber, the melting enthalpy ($\Delta H_{m\text{-pu}}$) obviously decreased with the increment of PC content in the PU/PC composite nanofibers. This may contribute to the intermolecular hydrogen bonding interaction between carbonyl groups of PC and amide groups of PU (Scheme 1). Such interaction may restrict the segment movement of PU molecular chains, and

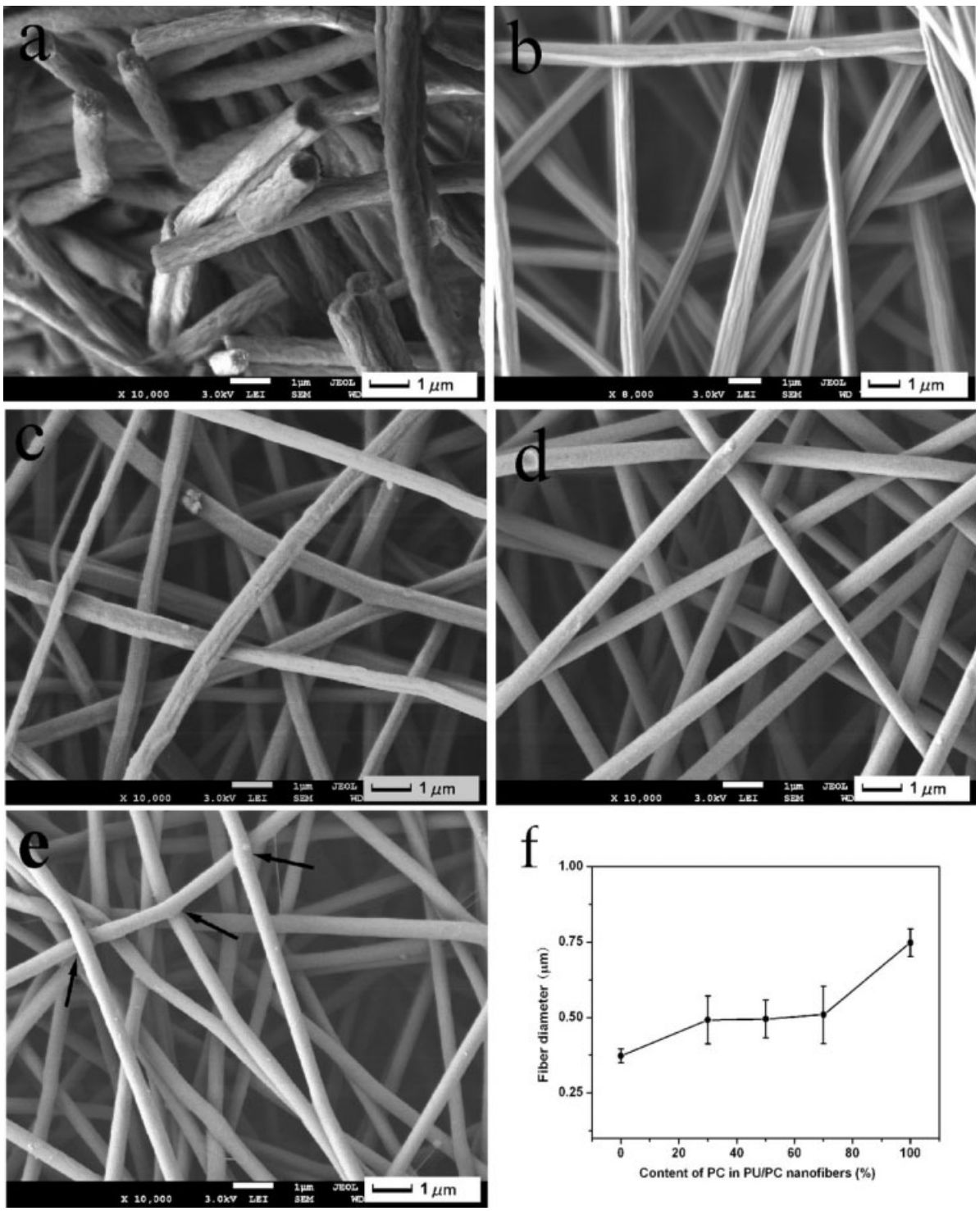

Figure 1 SEM images of PU/PC nanofibers (a) 0/100, (b) 30/70, (c) 50/50, (d) 70/30, and (e) 100/0; (f) diameter of corresponding nanofibers.

results in reduction of the crystallinity of PU phase (χ_c %) in the composite fiber (Table II). Thus, the melting enthalpy ($\Delta H_{m\text{-pu}}$) obviously decreased with increment of PC content in the PU/PC composite nanofibers.[22] This is in well agreement with their nanomorphology after removal of PC as suggested by the SEM and TEM analysis (discussed in the later section).

Thermal stability of PU/PC composite nanofibrous mat was investigated by thermogravimetric analysis. TGA thermograms of PU/PC composite nanofibers are presented in Figure 3. The decomposition

TABLE I
Solution Properties of PU/PC Dissolved in a Mixture of DMF/THF (30/70, v/v)

PU/PC	γ (m*N*/m) at 23°C	η (cp) at 25°C	Conductivity (μs/cm)
0/100	35.08	0.067	7.15
30/70	34.62	0.169	7.22
50/50	35.00	0.447	7.42
70/30	35.83	0.904	7.78
100/0	35.50	2.366	35.2

temperature (T_d) of PU and PC appeared at 306 and 370°C, respectively. No obvious change in the T_d of PU was found. However, the T_d of PC increases slightly when compared with that of pure PC nanofibers (Table II). The 50% weight loss temperature ($T_{50wt\%}$) for each sample is listed in Table II. It is shown that the PU/PC composite nanofibrous mat with higher content of PC has a larger $T_{50wt\%}$. Because PC is more thermal stable than PU, the thermal stability of PU fiber can be improved by compositing with PC.

The FTIR spectrum of the PU fibers had a strong stretching vibration (ν_{N-H}) at 3329 cm^{-1}, double peaks at 1731 and 1704 cm^{-1} for acrylamido ester group (*R*—O—C(=O)—NHR). The PC fibers exhibited a strong peak at 1770 cm^{-1} attributed to the stretching vibration of carbonyl group (*R*—O—C(=O)—O—R). In the FTIR spectrum of 50/50 PU/PC composite nanofibers, characteristic peaks of both PU and PC remained the same as observed in their single component counterparts [Fig. 4(a)], suggesting no strong interaction between PU and PC in the composite fibers.

Morphologies of PU/PC composite nanofibers after removal of PC

So far, distribution morphologies, such as cocontinuous,[14] islands-in-the-sea,[23] and core sheath[15] have been reported. Selective removal of one component followed by microscopical analysis is a very effective technique to uncover the information on the internal morphology of composite fibers, that is, how each component distributes within the composite nanofibers. The selective removal of the PC in the PU/PC

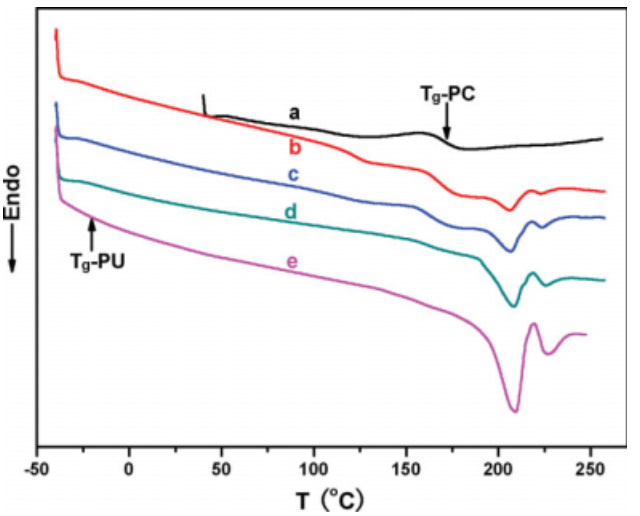

Figure 2 DSC curves of PU/PC composite nanofibers: (a) 100/0, (b) 70/30, (c) 50/50, (d) 30/70, and (e) 0/100. [Color figure can be viewed in the online issue, which is available at www.interscience.wiley.com.]

composite nanofibers was attempted by acetone immersion. This process caused 28.71, 42.57, and 67.39% mass loss for the composite nanofibers that originally contained 30, 50, and 70% of PC, respectively. The close match of mass loss to the theoretical PC content suggested that most PC was removed by acetone immersion. The removal of PC in these fibers was further verified by FTIR. The FTIR of 50/50 PU/PC nanofibrous mats showed very strong carbonyl stretching vibration of PC(*R*—O—C(=O)—O—R) peak at 1770 cm^{-1}. The acetone-treated fibers showed very weak peak at 1770 cm^{-1} [Fig. 4(b)]. Both the FTIR spectrum and weight loss value showed that PC was almost removed from composite nanofibers under prescribed conditions.

Figure 5 shows SEM photographs of PU/PC nanofibers after washed with acetone. For PU/PC 70/30 composite nanofibers after washed with acetone for 24 h, the residual PU fiber morphology was kept unchanged and also with smooth surface [Fig. 5(a)]. However, the surface of acetone-treated PU/PC 50/50 composite nanofibers was rough. Moreover, the fiber became distorted, elongated indents, and ridges along the fiber surface were also observed. The elongated indents were a few tens of nanometer wide

TABLE II
Thermal and Crystallinity Behaviors of PU/PC Composite Nanofibers

PU/PC	$T_{g\text{-pu}}$ (°C)	$T_{g\text{-pc}}$ (°C)	$T_{m\text{-pu}}$ (°C)	$\Delta H_{m\text{-pu}}$ ($J \cdot g^{-1}$)	$T_{d\text{-pu}}$ (°C)	$T_{d\text{-pc}}$ (°C)	Temp at 50% weight loss	Crystallinity of PU χ_c %
0/100	–	169.28	–	–	–	370	396	–
30/70	−24.96	168.23	206.29	11.28	307	373	396	13.4
50/50	−25.72	165.04	206.72	12.82	310	384	391	14.5
70/30	−26.05	161.21	208.08	15.33	307	385	383	16.1
100/0	−28.19	–	209.24	24.34	306	–	362	20.2

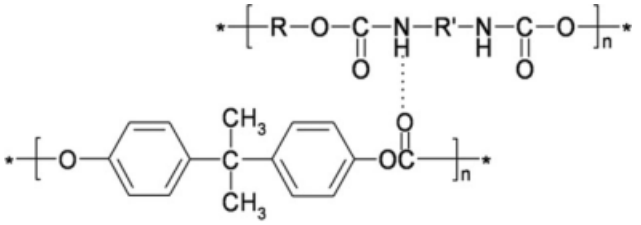

Scheme 1 Interaction between carbonyl and amide groups of PU and PC through hydrogen bonding.

and hundreds of nanometer long. In addition, fine features with nanometer size domains were observed on the fiber surfaces. As for acetone-treated 30/70 PU/PC composite fibers, this phenomenon became more obvious. The fiber became extremely nonuniform with lots of big pores. These differences on fiber surfaces between the two compositions suggested that the size and distribution of PC domains were PC content dependent. At low PC content, the PC domains were small and evenly dispersed in composite nanofibers. However, the small domains coexisted with the larger elongated domains with gradually increasing the PC content in the composite. Similar observations have been reported in the preparation of PEO/PAN

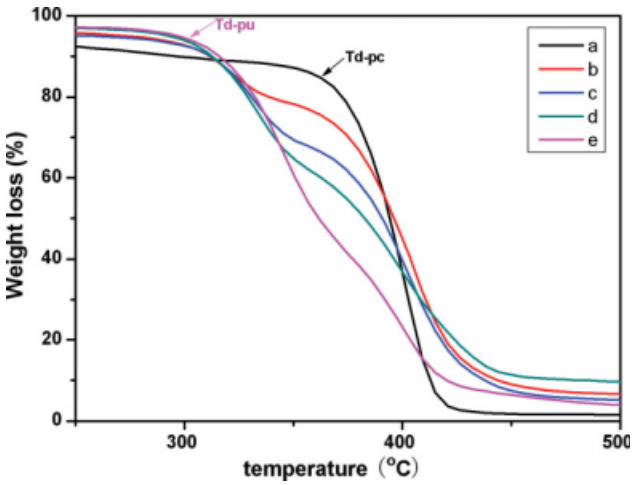

Figure 3 TGA curves of PU/PC composite nanofibers (a) 0/100, (b) 30/70, (c) 50/50, (d) 70/30, and (e) 100/0. [Color figure can be viewed in the online issue, which is available at www.interscience.wiley.com.]

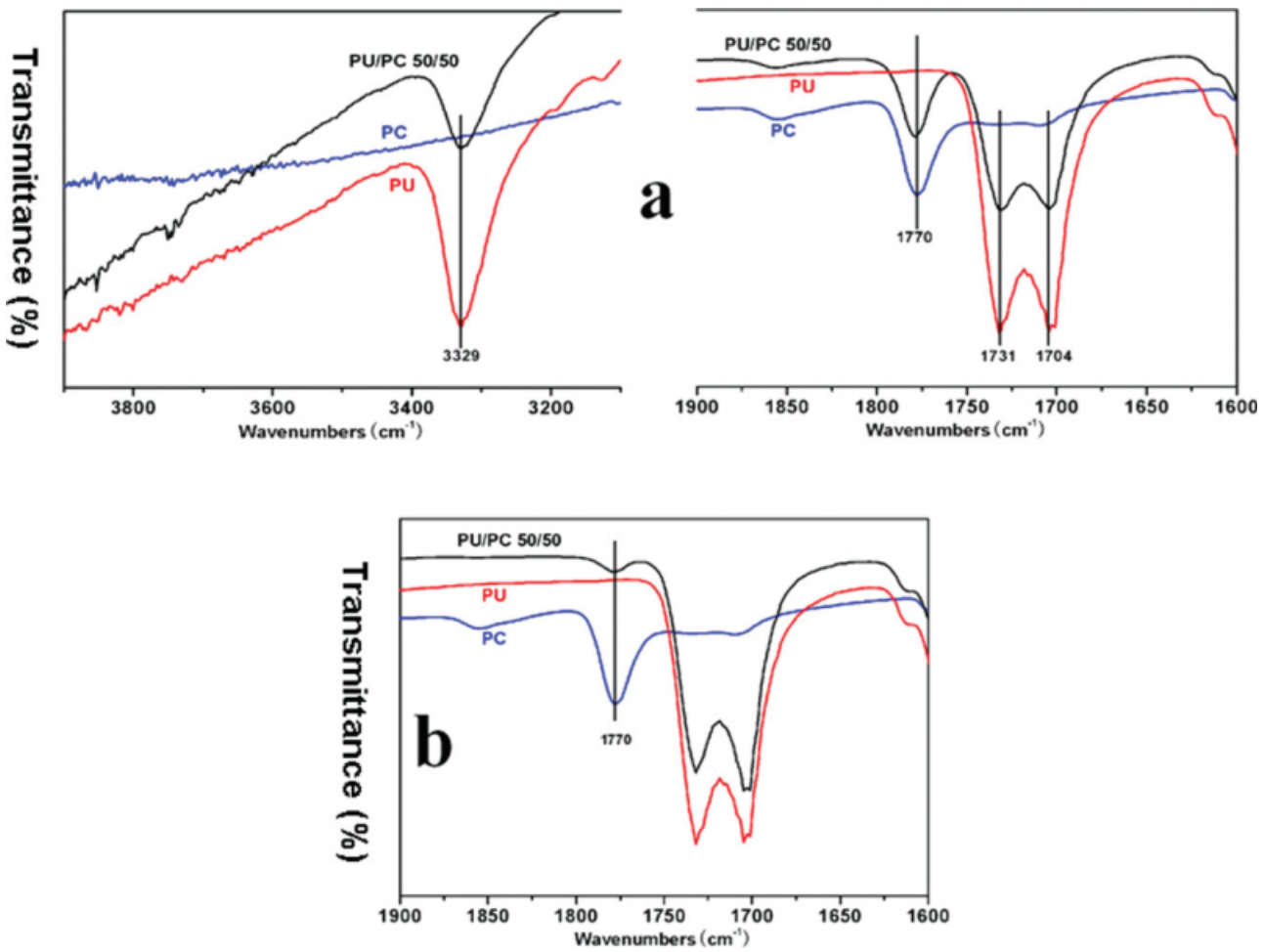

Figure 4 FTIR spectra of PU/PC nanofibers (a) as-electrospun and (b) after washed with acetone. [Color figure can be viewed in the online issue, which is available at www.interscience.wiley.com.]

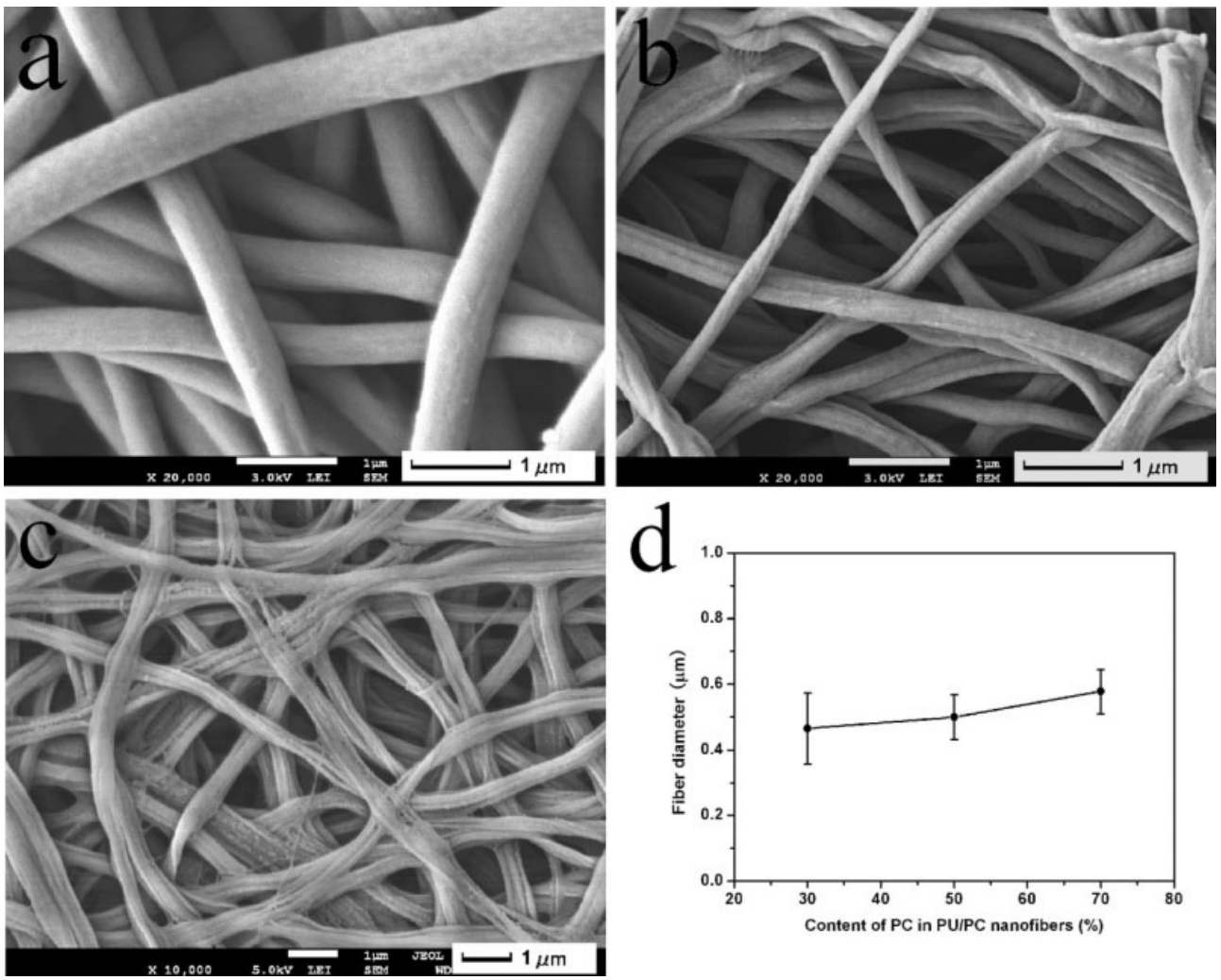

Figure 5 SEM images of PU/PC nanofibers after washed with acetone (a) 70/30, (b) 50/50, (c) 30/70, and (d) diameter of corresponding nanofibers.

bicomponent nanofibers.[23] Fiber size analysis from the SEM images showed that fiber diameters were kept unchanged after the removal of PC [Fig. 5(d)].

The smooth surface of 30/70 PU/PC composite nanofibers were clearly demonstrated in TEM image [Fig. 6(a)]. After the removal of PC, the surface of residual PU nanofibers becomes very coarse with shallow and elongated indents with several tens of nanometers in width (pointed by the arrows) were observed [Fig. 6(b)].

Mechanical properties of PU/PC composite nanofibrous mats

The typical stress–strain relationship of PU/PC composite nanofibers mats is shown in Figure 7. Unlike smooth stress–strain curve for bulk material such as cast film, characteristic seesaw curves are presented for nanofibrous mat attributed to the readily slipping and quickly reorientation of short nanofibers in the loosely packed isotropic nanofibrous mats during stretching. A similar phenomenon was observed in our previous work in the preparation of cocontinuous CA/PU composite nanofibers.[14] The pure PC and 30/70 PU/PC nanofibers were not showed in the Figure 7, because of these two fibers especially the pure PC fibers were extremely brittle [Fig. 1(a,b)] and discontinuous. Compared with the PU/PC 50/50, the curves of those mats with high PU content such as PU/PC 70/30, and 100/0 are in better shape, mainly because the bonding sites [Fig. 1(e)] among PU nanofibers keep them more integral than the loosely packed PU/PC 50/50 mats.

The mechanical properties of PU/PC nanofibrous mats were summarized in Table III. Comparing with the mechanical properties of pure PU nanofibrous mats, the presence of 30% PC in the PU/PC 70/30 significantly increased its modulus to more than 4-folds of pure PU nanofibers, while without much loss of tensile strength and elongation at break. This suggests that the rigid PC molecular chains enhance the rigidity of PU/PC nanofibrous mats. Although

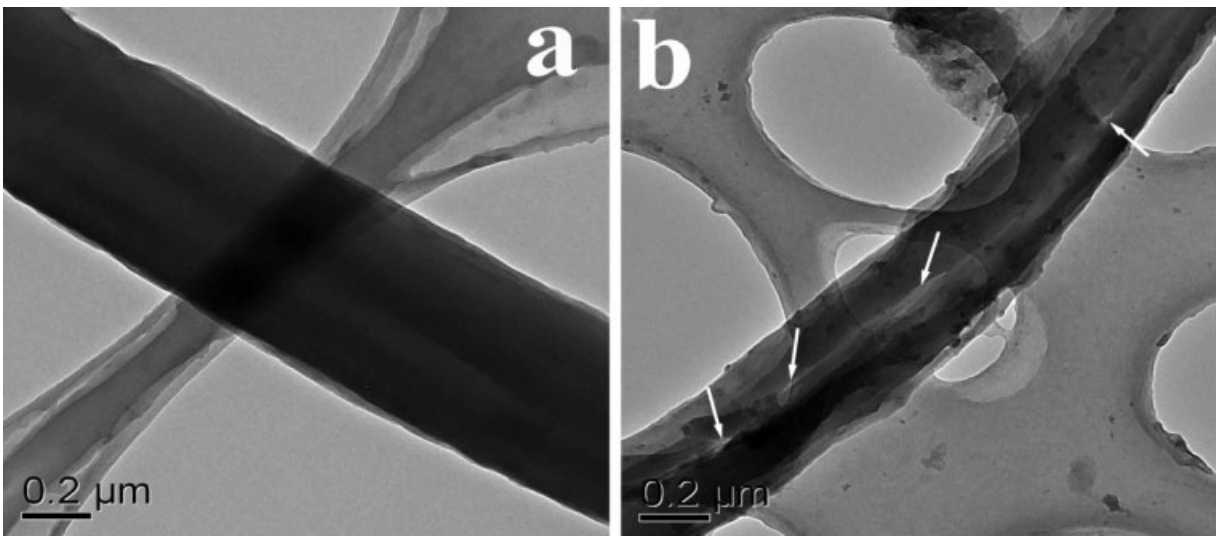

Figure 6 TEM images of PU/PC (30/70) nanofibers (a) as-electrospun and (b) after washed with acetone.

PU/PC 70/30 has similar fiber diameter to PU/PC 50/50, its yield strength and Young's modulus increased substantially to 9.6 MPa and 55 MPa, respectively. Because the content of PC is above 50% in the composite nanofiber, the PC phase became big, resulting in the concentration of stress in the PC phase, thus causing brittle fracture. The mechanical properties of electrospinning composite nanofibers mats were strongly influenced by the properties of each component in the composite nanofiber mats, nanofiber structure, and the interaction between each component.[20] In the case of the PC (shell)/PU (core) nanofibrous mats from coaxial electrospinning, the tensile behavior of the PC (shell)/PU (core) nanofibrous mats was enhanced with the increasing concentration of the PU (core) in the polymer solution.[12] Han realized that this could be due to the difference in the morphologies, as their shell materials were the same, whereas the core could contributed much to the mechanical performances. However, mechanical properties of PC (shell)/PU (core) composite nanofibrous mats are very poor, with yield strength (σ_y) and Young's modulus (E) of 0.33–0.82 MPa and 6–13 MPa, respectively. Therefore, compared with the coaxial of shell/core composite nanofiber, sea-island PC/PU composite nanofiber obtained in our work can largely improve its mechanical properties

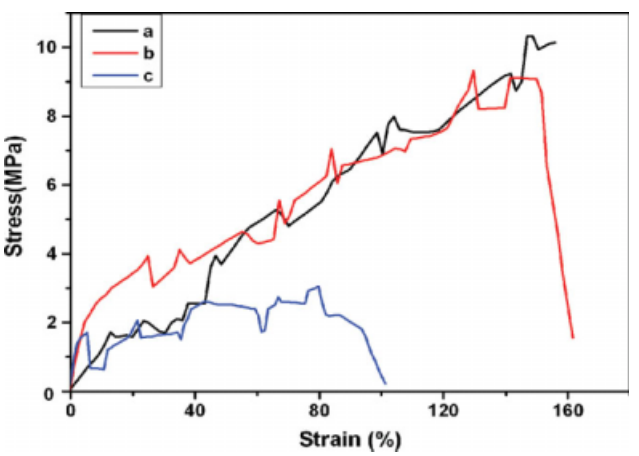

Figure 7 Stress–strain curves of PU/PC nanofibrous membranes (a) 100/0, (b) 70/30, and (c) 50/50. [Color figure can be viewed in the online issue, which is available at www.interscience.wiley.com.]

Phase distribution model in PU/PC composite nanofibers

Based on the morphology, structure, thermal behaviors, and the mechanical properties, the distribution model of PC phase in PU/PC composite nanofibers is presented in Figure 8. These difference such as the surfaces of fibers before and after acetone treatment, thermal behaviors (T_g, ΔH_m), and the mechanical properties with different content of the two component suggested that the size and the distribution of PC domains were PC content dependent. The PC domains were small and evenly dispersed as irregular domains in the PU/PC composite nanofibers with low PC content. As PC content increased in composite fibers, small irregular domains coexisted with the larger elongated domains. The latter was

TABLE III
Mechanical Properties of PU/PC Nanofibrous Membranes

PU/PC	σ_y (MPa)	ε_b (%)	E (MPa)
100/0	9.9 ± 1.9	119 ± 15	13 ± 6
70/30	9.6 ± 1.2	122 ± 18	55 ± 16
50/50	4.9 ± 0.5	85 ± 6	37 ± 10

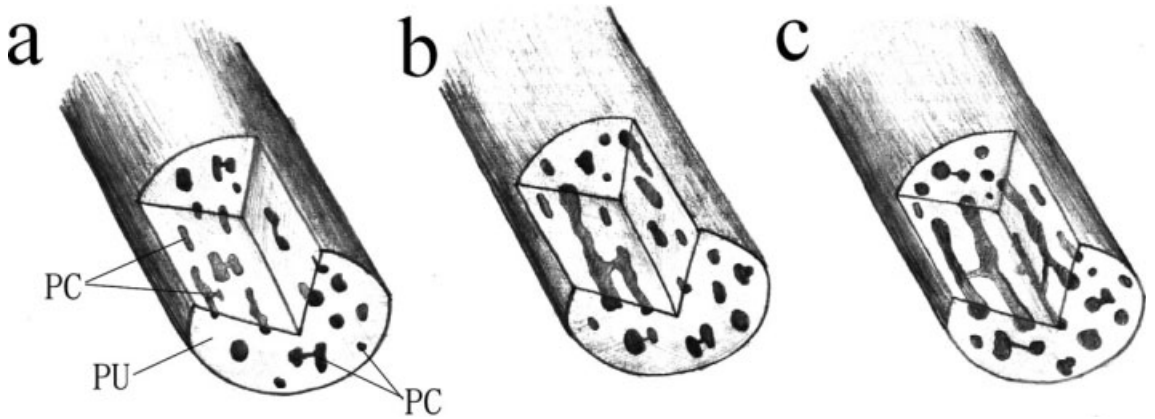

Figure 8 PC phase distribution model in PU/PC composite nanofibers: (a) 70/30, (b) 50/50, and (c) 30/70.

from the merger of the former. Therefore, the phase distribution of PU/PC was typical the sea-island structure. This phenomenon is due to phase separation in the spinning solution and in the course of electrospinning.[24]

CONCLUSIONS

In this study, PU/PC composite nanofibers in a broad range of composite ratios were prepared through electrospinning. Phase separation in the composite nanofibers was confirmed by FTIR, DSC, and TGA analyses. The removal of the PC domains by acetone immersion was confirmed by FTIR, SEM, TEM, and weight loss data, suggesting the size and the distribution of PC domains in the composite were PC content dependent. Compared with the PU or PC fiber, PU/PC composite nanofibers overcome the weak points of each component such as low tensile strength of PC, high strain and low modulus of PU, while combine strong points to improve its whole mechanical properties. Moreover, the thermal stability of PU fiber can be improved by adding a certain amount of PC. On basis of the morphology, structure, thermal behavior, and the mechanical properties, the PC phase distribution model in PU/PC composite nanofibers is defined to be sea-island structure.

References

1. Appenzeller, J.; Radosavljevi, M.; Knoch, J.; Avouris, P. Phys Rev Lett 2004, 92, 48301.
2. Xia, Y.; Yang, P.; Sun, Y.; Wu, Y.; Mayers, B.; Gates, B.; Yin, Y.; Kim, F.; Yan, H. Adv Mater 2003, 15, 353.
3. Subbiah, T.; Bhat, G. S.; Tock, R. W.; Parameswaran, S.; Ramkumar, S. S. J Appl Polym Sci 2005, 96, 557.
4. Doshi, J.; Reneker, D. H. J Electrostat 1995, 35, 151.
5. Gibson, P.; Schreuder-Gibson, H.; Rivin, D. Colloids Surf A 2001, 187, 469.
6. Mo, X. M.; Xu, C. Y.; Kotaki, M.; Ramakrishna, S. Biomaterials 2004, 25, 1883.
7. Norris, I. D.; Shaker, M. M.; Ko, F. K.; MacDiarmid, A. G. Synth Met 2000, 114, 109.
8. Ding, B.; Kimura, E.; Sato, T.; Fujita, S.; Shiratori, S. Polymer 2004, 45, 1895.
9. Theron, S. A.; Yarin, A. L.; Zussman, E.; Kroll, E. Polymer 2005, 46, 2889.
10. Gupta, P.; Wilkes, G. L. Polymer 2003, 44, 6353.
11. Liu, Z.; Sun, D. D.; Guo, P.; Leckie, J. O. Nano Lett 2007, 7, 1081.
12. Han, X. J.; Huang, Z. M.; He, C. L.; Liu, L.; Wu, Q. S. Polym Compos 2006, 27, 381.
13. Song, T.; Zhang, Y.; Zhou, T.; Lim, C. T.; Ramakrishna, S.; Liu, B. Chem Phys Lett 2005, 415, 317.
14. Tang, C.; Chen, P.; Liu, H. Polym Eng Sci 2008, 48, 1296.
15. Wei, M.; Lee, J.; Kang, B.; Mead, J. Macromol Rapid Commun 2005, 26, 1127.
16. Jin, H. J.; Fridrikh, S. V.; Rutledge, G. C.; Kaplan, D. L. Biomacromolecules 2002, 3, 1233.
17. Park, K. E.; Jung, S. Y.; Lee, S. J.; Min, B. M.; Park, W. H. Int J Biol Macromol 2006, 38, 165.
18. Moon, S.; Farris, R. J. Polym Eng Sci 2008, 48, 1848.
19. Demir, M. M.; Yilgor, I.; Yilgor, E.; Erman, B. Polymer 2002, 43, 3303.
20. Lee, K. H.; Kim, H. Y.; Ryu, Y. J.; Kim, K. W.; Choi, S. W. J Polym Sci Part B: Polym Phys 2003, 41, 1256.
21. Koombhongse, S.; Liu, W.; Reneker, D. H. J Polym Sci Part B: Polym Phys 2001, 39, 2598.
22. Bradley, A. E.; Hardacre, C.; Holbrey, J. D.; Johnston, S.; McMath, S. E. J.; Nieuwenhuyzen, M. Chem Mater 2002, 14, 629.
23. Zhang, L.; Hsieh, Y. Nanotechnology 2006, 17, 4416.
24. Bognitzki, M.; Frese, T.; Steinhart, M.; Greiner, A.; Wendorff, J. H.; Schaper, A.; Hellwig, M. Polym Eng Sci 2001, 41, 982.